

# Unlocking the Potential of Robotic Solutions to Calibrate and Measure Active Electronically Scanned Arrays

*by Patrick Pelland and Daniël Janse van Rensburg*



## INTRODUCTION

Phased array, and more specifically Active Electronically Scanned Array (AESA) technology has been in use for several decades. This type of array uses active components to control the phase and amplitude weighting of individual elements or groups of elements to modify the array's aperture distribution. The result is that the effective radiation pattern of the array can be controlled and reconfigured at a rate that is supported by the electronics. In the past, the cost and complexity of developing, manufacturing, and testing these arrays made the technology mostly inaccessible for non-military applications. Technological advances in the RF components used to build up phased arrays have led to more cost effective and miniaturized solutions. This, combined with a broader understanding of the theory and best practices regarding phased array design, makes the technology viable across many industries including automotive, communication, medical and commercial aerospace. As a result of their proliferation, the need to accurately calibrate and measure AESA performance is on the rise.

Industrial robots are becoming increasingly popular for use in antenna measurement systems [1] - [3]. These devices are relatively inexpensive, offer highly repeatable mechanical performance and are very reliable. These versatile robots can also be reconfigured to support multiple different measurement geometries, which make them ideal for use in antenna measurement systems. The acceleration and settling time of these industrial robots are unmatched by other mechanical positioners, so they are ideally suited for applications where a probe antenna must move from one point to another as efficiently as possible. This has proven useful for phased array calibration. This article describes a typical calibration and measurement process with two robotic based measurement facilities currently under development.

# MEASUREMENT AND CALIBRATION OF PHASED ARRAYS

Radiation measurements for phased arrays can be broadly split into three main categories: *element pattern characterization*, *array calibration* and *array far-field pattern measurements*.

## Element Pattern Characterization

This step involves measuring one or more of the individual elements that make up the array. Assuming all elements in the array are identical, the element radiation pattern, multiplied with the array factor [4] will yield the phased array pattern. As such, it is important to validate the performance of one or more elements prior to assembling the elements into an array or sub-array module.

Since these elements tend to have fairly broad radiation patterns, it is preferred to measure them on a test system that can provide complete front hemisphere performance, at a minimum. Suitable systems that meet these criteria are direct illumination Far-Field (FF) solutions, Compact Antenna Test Ranges (CATR) or Spherical Near-Field (SNF) ranges [5]. Due to their smaller footprint and cost, SNF testing is often the preferred approach to this type of element characterization. These techniques rely on measuring the antenna's response in the near field and mathematically transforming it to the far field. Robotic systems can also be used to implement a SNF test solution. The examples described in [1] and [2] are suitable solutions that use the type of industrial robot being considered here, with an example of one such system shown in the figure to the right. The Antenna Under Test (AUT) rotates about a vertical  $\phi$ -axis, implemented by the floor mounted rotary stage. The six-axis robot moves a near-field probe along a circular arc to create a virtual  $\theta$ -axis of motion. The combination of these two axes allows data to be acquired over a partial sphere enclosing the AUT.



Figure 1: Robotic scanner used for spherical near-field measurements

Further space efficiency can be realized by considering non-canonical acquisition surfaces too. The measurement system described in [3] uses a capped cylindrical measurement geometry and a non-canonical near-field to far-field transformation to support the same type of element characterization. Both near-field solutions offer radiation pattern coverage over more than a hemisphere.

Once element patterns have been verified, the AESA integration and assembly can proceed, and an array calibration process is required.

## Array Calibration

An AESA uses active electronics to allow for high-speed radiation pattern reconfiguration. Each radiating element (or sub-array collection of elements) will be connected to a phase shifter or time delay device used to adjust the relative phases at the output of these elements. This allows the array to synthesize a tilted phase front to effectively steer the main beam to a desired look angle. More complex phased arrays might also have the ability to control the relative amplitudes of the elements to also alter the aperture power distribution, as depicted on the right. This allows for main

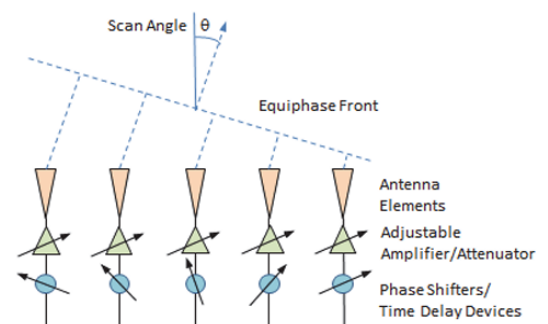


Figure 2: Simplified phased array antenna architecture [6]

beam directivity and pattern side lobe control and/or pattern null steering. (Very large AESAs can also consist of sub-array units, sometimes called tiles, that are calibrated separately before being combined to form the full array. These tiles are often pre-calibrated before integration into the larger array.) A simplified phased array schematic with both amplitude and phase adjustment is shown in Figure 2.

Before the array can be operationally exercised through its various beam states, the relative amplitude and phase of each element and its RF path must be characterized. This process is known as inter-element calibration or tuning. This process must include the contribution of the radiating element, so it should be conducted using a radiated setup, like an antenna measurement system. The ideal tuning scenario is depicted in Figure 3, showing an array of  $N$  elements. In this example, the array is illuminated by a perfect plane wave from an ideal measurement system. The amplitude and phase are recorded at each element in turn. Next, the phase and amplitude are normalized so that the array is configured into its baseline state where the beam will be steered to boresight. (Since components are frequency sensitive and typically non-linear, this process must be conducted at all frequencies of interest and across many different power levels.) From here, custom beam patterns can be synthesized by adjusting element weighting relative to the calibrated baseline.

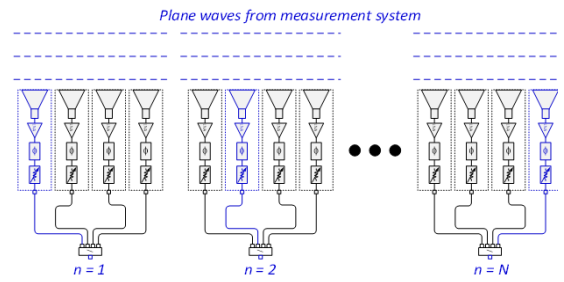


Figure 3: Phased array illuminated by an ideal plane wave

This ideal measurement scenario is approximated in practice. CATR and FF systems are designed so that a volume in space is illuminated by a pseudo plane wave. This region is called the Quiet Zone (QZ) [5]. This pseudo plane wave, while acceptable for antenna radiation pattern characterization, can exhibit peak-to-peak variations on the order of  $\pm 0.5$  dB in amplitude and  $\pm 10^\circ$  in phase throughout its volume and as a result, the wavefront illuminating the AESA is imperfect. This test environment will result in varying amplitude and phase illumination of the array elements, which becomes a calibration uncertainty or should otherwise be compensated for.

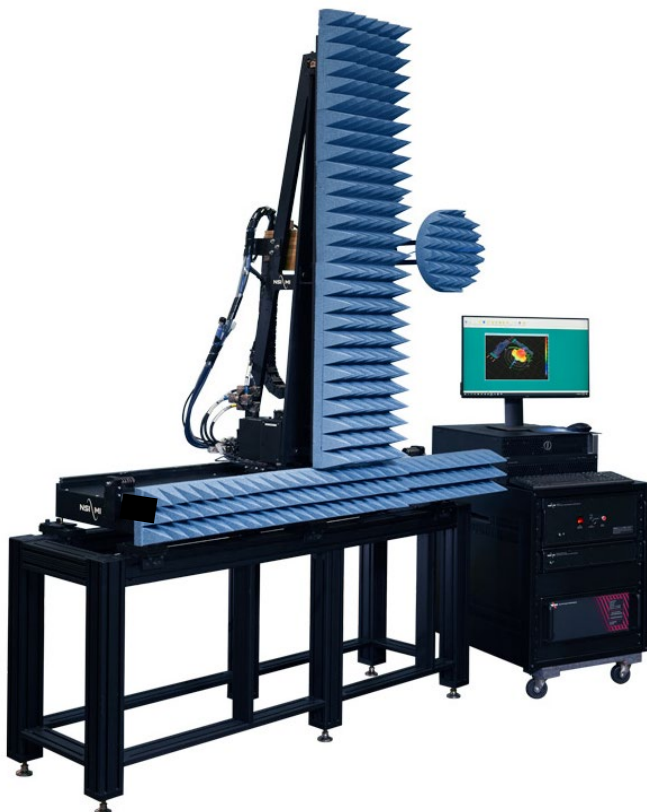


Figure 4: Vertical PNF measurement system with 0.9m x 0.9m scan plane

Rather than attempting to compensate for field imperfections in the system illuminating the AESA, one can instead change the relative positions between the AESA and a known field point such that every element is illuminated identically. This reduces the impact of the imperfection of the illuminating field on the array calibration since each element will see the same incoming signal.

For the CATR solution, one can place two orthogonal, linear axes behind the AESA to move each element to the center of the QZ for RF path calibration of that element and this would largely eliminate the need to perform QZ compensation. However, this approach becomes increasingly cost and size prohibitive as the AESA dimensions grow. In practice, a planar near-field (PNF) measurement geometry is often used for this task. Like the SNF solution previously discussed, PNF measurement systems rely on acquiring data in the AUT's

near-field and mathematically transforming it to the far field. While the SNF system collects data in a complete or partial spherical surface, the PNF geometry relies on data collection on a planar surface in the AUT's forward hemisphere. An example of one such PNF measurement system is shown in Figure 4. A graphical depiction of the PNF vertical acquisition surface with the probe scanning along the vertical axis is shown in Figure 5.

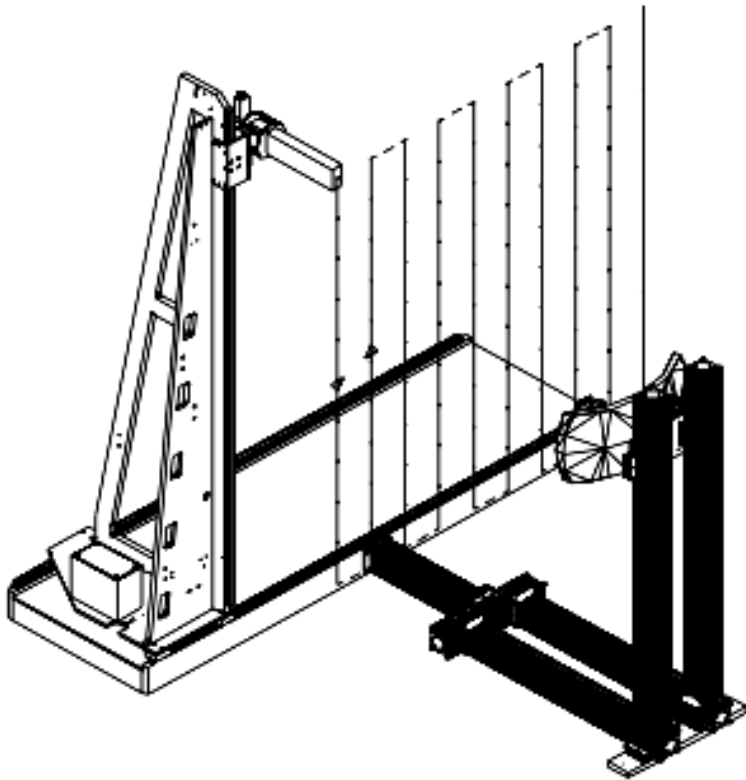


Figure 5: Depiction of vertical PNF scan plane with probe scanning along vertical axis and stepping horizontally.

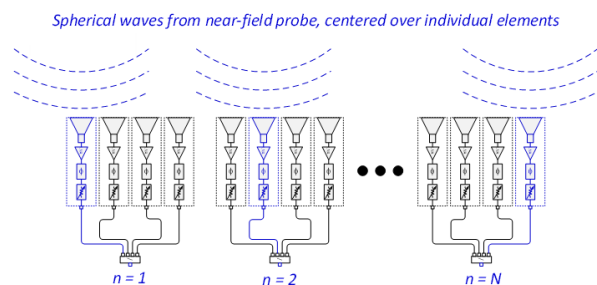


Figure 6: Phased array individual elements illuminated by spherical waves emanating from near-field probe on PNF test system.

For element level phased array calibration, one is only interested in the system's ability to precisely position a probe in front of each array element, transmit and/or receive RF energy, and store the collected amplitude and phase data. This process is often called a *park & probe* measurement. The park & probe process is depicted in Figure 6. The incoming wave exciting the elements at each probe position is spherical, but the non-ideal probe effects will be the same for each RF path and can therefore be ignored.

Upon completion of this data collection (for all array elements, all frequencies and power levels), the measured data are transferred to the AESA controller and algorithms (often proprietary and customer specific) will be used to calculate the AESA calibration matrix to establish the baseline settings. This process is typically iterative and often requires multiple calibration passes. In practice, there are mitigating uncertainty factors to consider:

#### Temperature and Flex Cable Variation

Many AESAs must support operation over a wide temperature range. For these cases, temperature becomes a measurement parameter in the calibration process. Once the AESA's temperature dependence is well-understood, testing conditions can be relaxed with some temperature normalization applied to the calibration data. Of course, the PNF measurement system will also be sensitive to temperature variation and RF flex cable stability, so care must be taken to ensure phase errors are not introduced by the test system.

Since PNF testing could span a lengthy time period, temperature drift of the environment during the course of calibration should be considered. If the temperature cannot be kept sufficiently stable, the effects of unwanted temperature drift should be monitored and compensated for [7], [8].

### *Frequency and RF Power*

The calibration of an AESA will be frequency and power dependent, so measurements must be performed at multiple discrete frequencies and power levels. The density of the data points required for calibration can vary greatly from one AESA to the next and this should be carefully considered. This does not usually represent a significant obstacle, given the speed and accuracy of modern RF sub-systems but it can present a test time challenge.

### *Element Mutual Coupling*

Array element mutual coupling typically drive an iterative approach to the element level calibration process. This is because a single element (and its associated active electronics) will be impacted differently depending on the excitation of its neighbors. For an initial pass, rather than activate all array elements, many calibration algorithms rely on exciting only the element under test, along with a limited number of adjacent elements. Once the first calibration pass has been completed, a better picture of actual element excitation is known and the process can be repeated for a second pass to approach an environment closer to real operating conditions. AESA inter-element mutual coupling can be addressed in different ways as described in [6] & [9].

Upon completion of the array calibration, far-field pattern characterization needs to be performed.

### *Array Far-Field Pattern Measurements*

Due to their complex performance AESAs must be tested in multiple beam configurations, achieved by strategically adjusting the AESA's active components to alter the aperture distribution. The need to test over multiple beam states places more restrictions on the type of measurement system required to test AESAs and here PNF solutions are often called upon. A PNF solution is suitable for cases where the main beam is scanned up to 60° from boresight, but SNF systems are required when greater angular coverage must be measured. In both cases a robotic solution can be used to implement these solutions.

## ROBOTIC MEASUREMENT SOLUTIONS

Two robotic antenna measurement systems being deployed for AESA characterization are described in this section. The AESA considered, consists of several individually calibrated sub-array tiles which then get assembled to form the full array. The tiles are calibrated using a tuning station, while the assembled array's full beam patterns are characterized using the measurement system.

### *Sub-Array Tuning Station*

To address the need for sub-array tile tuning, the system shown in Figure 7 is being developed. This system uses a 6-axis industrial robot integrated onto a portable base for park & probe measurements. All RF and control equipment is mounted within the enclosure, behind the robot base. The tiles are mounted onto a fixture with precision locating pins to guarantee test article alignment to within  $\Delta X, \Delta Y \leq \pm 0.025\text{mm}$ . Precision machined mounting surfaces on both the test station and tile base

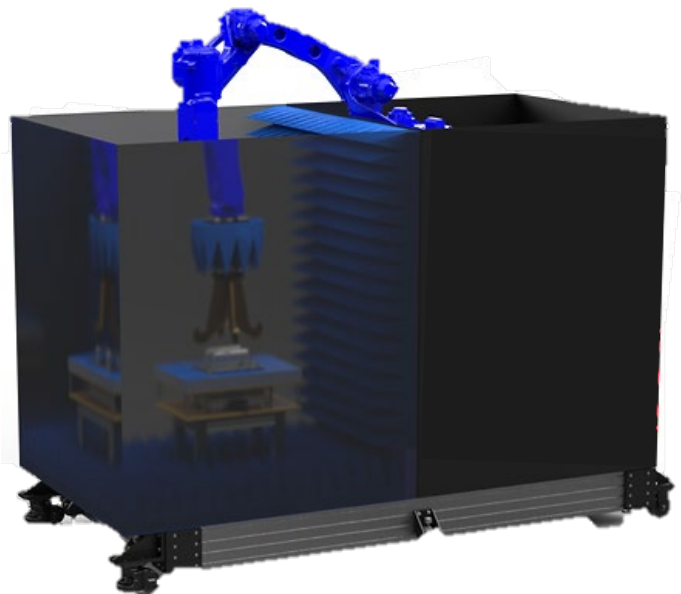


*Figure 7: Robot-based tuning station for high throughput production testing of sub-array tiles*

ensure AESA coplanarity with the measurement system scan plane to within  $\pm 0.01^\circ$ . The robot will move a broadband probe to each element and execute an iterative calibration routine. When calibration has concluded, the probe will move to a fixed point above the array for a health check of the tile's RF radiation. Some critical details of the tuning station are shown in the table below.

Parameter	Value
Maximum Calibration Area	610 mm x 610 mm
Positioning Repeatability	0.02 mm
Probe Bandwidth	1 – 15 GHz
Frequency Switching Speed	40 $\mu$ s
Probe to AESA Spacing	110 mm $\leq z \leq$ 910 mm
AESA Alignment	Locating Pins and Machined Surfaces
Total System Envelope	3.27 m (L) x 1.34 m (W) x 2.67 m (H)

### Full Array Measurement System

After calibration of all sub-array tiles the full array is assembled and ready for pattern measurement. The AESA described is mounted on a trailer and tilted at  $45^\circ$  from vertical. To accommodate this large, tilted array, the robotic measurement system shown to the right was designed. The robot holding the near-field probe is mounted on a precision linear axis to achieve a maximum scan plane size of 9.1m x 5.5 m, tilted to match the array aperture. An Automatic Probe Changer (APC) system houses several near-field probes and accessories to support measurements over a wide frequency range.

The array is moved into location using a motorized cart and a pre-alignment is conducted using physical monuments in the chamber.

One of the APC accessories is a laser range finder, which allows the system to measure the relative distance between the AESA and scan plane. By measuring the distance to three reference points on the AESA, the coplanarity error of the AESA and scan plane can be calculated. The measurement system will then automatically compensate for this error to ensure accurate beam pointing measurements for the full array.

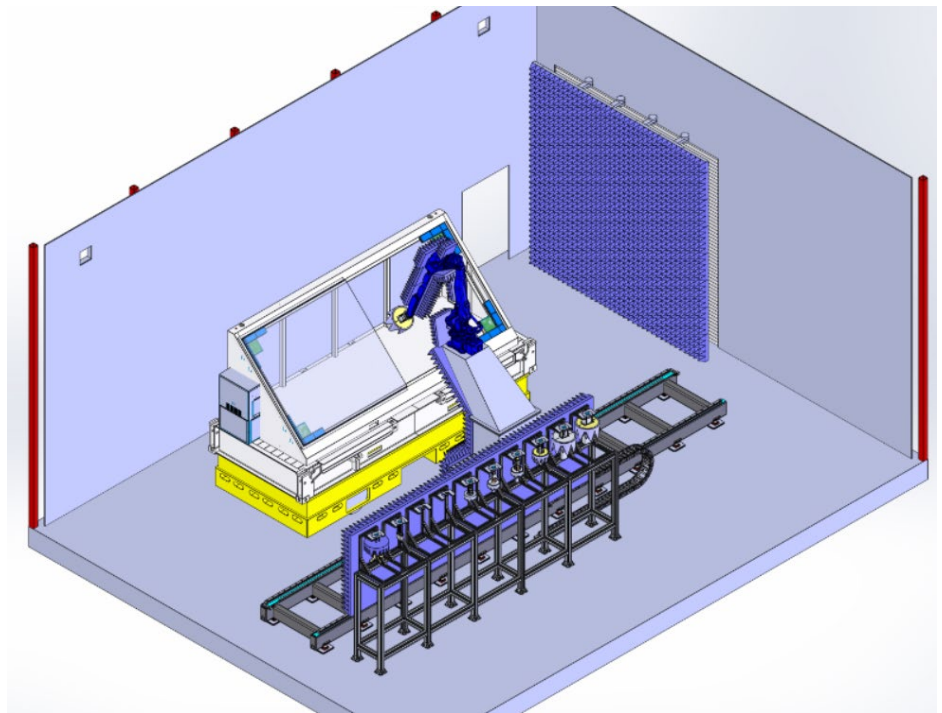


Figure 8: Robotic AESA Measurement System with 9.1 m x 5.5 m scan plane tilted at  $45^\circ$  from vertical.

# CONCLUSION

The proliferation of AESA technology has led to an increased demand for suitable RF measurement solutions and robotic systems offer that unique capability. We show here how all the stages of AESA testing and calibration can be addressed. Although not explicitly described here, complicating factors like internal AESA frequency conversion, radiated power density and the implication on safety, digital data handling and measurement throughput, all form part of this test challenge and must be considered in these solutions.

# REFERENCES

- [1] D. Novotny, J. Gordon, J. Coder, M. Francis and J. Guerrieri, "Performance evaluation of a robotically controlled millimeter-wave near-field pattern range at NIST," *Antennas and Propagation (EuCap), 7th European Conference on Antennas and Propagation*, pp.4086 – 4089, 8-12 April 2013.
- [2] J. Hatzis, P. Pelland and G. Hindman, "Implementation of a combination planar and spherical near-field antenna measurement system using industrial 6-axis robot," *AMTA 38th Annual Meeting & Symposium, Austin TX, Oct 2016*.
- [3] D. Janse van Rensburg, B. Walkenhorst, Q. Ton and J. Demas, "A robotic near-field antenna test system relying on non-canonical transformation techniques," *AMTA 41st Annual Meeting & Symposium, San Diego CA, Oct. 2019*.
- [4] P. Bevelacqua. (2020) *The Array Factor*. *Antenna-Theory.com* [Online]. Available: <https://www.antenna-theory.com/arrays/arrayfactor.php>
- [5] C. Parini, S. Gregson, J. McCormick and D. Janse van Rensburg, *Theory and Practice of Modern Antenna Range Measurements*, The Institute of Engineering and Technology, London, UK, 2015.
- [6] K. Hassett, "Phased array antenna calibration measurement techniques and methods," *Antennas and Propagation (EuCap), 10th European Conference on Antennas and Propagation, 10-15 April 2016*.
- [7] K. Haner, G. Masters, "State-of-the-art near-field measurement system," *AMTA 17th Annual Meeting & Symposium, Nov. 1995*.
- [8] S. Bhatia, C. Huber, W. Dorsey, A. Sayers, "Measurement techniques for a transmit/receive digital phased array," *AMTA 33rd Annual Meeting & Symposium, Nov. 2011*.
- [9] M. Foegelle, "Simultaneous measurement of analog phased array elements using orthogonal coding," *AMTA 43rd Annual Meeting & Symposium, Nov. 2021*.